Journal of Cleaner Production 205 (2018) 955–963

Contents lists available at ScienceDirect

Journal of Cleaner Production

journal homepage: www.elsevier.com/locate/jclepro

Using hydrothermal carbonization for sustainable treatment and reuse of human excreta

Reut Yahav Spitzer, Vivian Mau, Amit Gross*

Department of Environmental Hydrology and Microbiology, Zuckerberg Institute for Water Research, Ben Gurion University of the Negev, Sde Boqer 84990, Israel

ARTICLE INFO

Article history:
Received 14 June 2018
Received in revised form
5 September 2018
Accepted 14 September 2018
Available online 17 September 2018

Keywords:
Black water
Hydrothermal carbonization
Human excreta
Sanitation technology
Solid biofuel
Liquid fertilizer

ABSTRACT

Poor sanitation due to improper treatment of human excreta, and energy scarcity are global problems with only partial solutions. Thus, feasible conversion of human excreta into safe, reusable "products" and renewable energy could be advantageous. The research objectives were to study the properties and major chemical processes occurring during hydrothermal carbonization of raw human excreta with typical solids content, as well as exploring potential use of the resulting hydrochar and aqueous phase. Human excreta (often considered as black water) were hydrothermally carbonized in a set of nine 50-mL laboratory batch reactors under a range of severities, a single parameter obtained from a coalification model that represents the combination of temperature and time. Three temperatures (180, 210 and 240 °C) and reaction times (30, 60 and 120 min) were used. The physicochemical characteristics such as yield, elemental composition, organic matter and calorific value of the hydrochar (solid phase) were studied. Aqueous phase was characterized for carbon, nitrogen, macro and micronutrients composition. In addition, the potential use of the hydrochar and aqueous phase were studied. There was high correlation between severity factor and carbon content ($R^2 = 0.95$) and calorific value ($R^2 = 0.89$). Hydrochar yield decreased with increasing severity from 69 to 56%. Calorific values increased from 24.7 to 27.6 MJ/kg, falling within the calorific range of sub-bituminous coal. The aqueous phase demonstrated high nitrogen concentration, reaching up to 8178 mg/L total nitrogen, while N:P:K ratios were similar to those of commercial fertilizers. Pilot scale experiments resembled the results found in laboratory scale experiments for both hydrochar and aqueous phase and fitted the regression curves obtained from the severity factor. It is postulated that hydrothermal carbonization of human excreta could potentially serve as a sustainable sanitation technology with a closed-loop cycle approach while recovering energy and nutrients.

1. Introduction

Poor sanitation and energy scarcity are big challenges in the developing world, contributing to health, environmental, economic and social problems. Around 2.3 billion people worldwide, mainly from developing countries, do not have access to safe sanitation facilities. Of these, 892 million still practice open defecation (WHO and UNICEF, 2017). Inadequate water, sanitation, and hygiene problems cause the death of around 842,000 people annually, 280,000 of which succumb to diarrheal death due to poor sanitation (WHO and UNICEF, 2017). Similarly, energy scarcity affects the poorest people. Around 2 billion people use solid biomass, especially wood which is collected and converted into wood-charcoal, to provide their energy needs, such as cooking and heating; these practices have environmental impacts, including air pollution, greenhouse gas emissions, deforestation, and soil erosion (Bailis et al., 2003; Ward et al., 2014).

Human excreta (often termed as black water) are considered hazardous due their potential to transmit diseases. They are also rich in organic matter and nutrients such as nitrogen, phosphorus and potassium, which can lead to environmental problems if not disposed properly. It is estimated that each person generates between 120 and 530 g of wet human feces and 1–1.4 L of urine per day (Rose et al., 2015). These nutrients can potentially be reused and recovered after appropriate treatment (Hu et al., 2016). Hydrothermal carbonization (HTC) could provide the necessary

* Corresponding author.
E-mail address: amgross@bgu.ac.il (A. Gross).

https://doi.org/10.1016/j.jclepro.2018.09.126
0959-6526/

treatment to recover nutrients and sterilize human excreta while addressing sanitation and energy problems.

HTC is a thermochemical process that typically ranges between a few minutes and several hours, in which wet biomass is heated to temperatures ranging from 180 to 250 °C and self-generated pressure maintains water in a subcritical state. During the process, mainly hydrolysis, decarboxylation and dehydration reactions occur, resulting in mass loss, mainly of oxygen and hydrogen molecules. As a result, a carbon-rich solid phase with high calorific value, referred to as hydrochar, a nutrient-rich aqueous phase and some excess gas are formed (Funke and Ziegler, 2010). HTC has the potential to become an attractive treatment alternative because (i) it enables relatively short processing times; (ii) the reaction sterilizes the products; (iii) significant degradation of micropollutants, such as endocrine-disrupting agents and pharmaceuticals, is expected (vom Eyser et al., 2015), and (iv) it is considered an energy-efficient technology (Ramke et al., 2009; Reißmann et al., 2018). Moreover, it could also be considered as a sustainable treatment with a closed-loop cycle approach that recovers energy and allows the reuse of nutrients.

Only a few studies have investigated human waste as HTC feedstock, and most of those focused on sewage sludge after different levels of treatment: Danso-Boateng et al. (2013, 2015b, 2015c) and Afolabi et al. (2015, 2017) investigated primary sewage sludge, while Escala et al. (2013) and Smith et al. (2016) investigated secondary sewage sludge and stabilized sludge after anaerobic digestion. Interestingly, in the few studies investigating HTC of human excreta (Afolabi et al., 2015, 2017), the excreta were diluted from their "typical" 20–25% solids content (Rose et al., 2015) to about 5% solids content by adding water, and reaction temperatures were up to 200 °C. Danso-Boateng et al. (2013, 2015b) used synthetic feces with solids contents of 5%, 15% and 25% subjected to 140–200 °C, and focused on the kinetics of hydrochar production and its properties.

The main objectives of this study were to explore the properties and major chemical processes occurring during HTC of raw human excreta with typical solids content (~25% solids) in a temperature range of 180, 210 and 240 °C. Specifically: (i) aqueous and solid phases were characterized for their physicochemical properties, (ii) mass balances of carbon and nitrogen were conducted, (iii) potential use of the aqueous phase as fertilizer was evaluated, (iv) an energy accounting was calculated to explore the relevance of this practice as a sustainable environmental solution, and (v) a pilot scale reactor was operated to validate the observations from laboratory experiments. This study is the first to investigate HTC of actual human excreta with its natural moisture content. Together with the pilot scale experiment, this research is able to represent the process as closely as possible to real-world application to date.

2. Materials and methods

Raw human excreta were collected from seven people. The participants defecated and urinated into pre-weighed autoclave bags attached to a dry field toilet unit (toilet paper was not introduced) and plastic bags were sealed. At the end of each day, the collected excreta bags were autoclaved to prevent possible infection and contamination by pathogens. Full bags were weighed, dried for 24 h at 105 °C and weighed again. The dry material was then pulverized in a mechanical grinder. The homogenized feedstock was stored in a desiccator prior to HTC experiments. Dry weight and water content ratios were calculated to wet the excreta to their initial water content prior to carbonization.

2.1. Carbonization experimental setup

HTC experiments were performed in a set of nine 50-mL laboratory batch reactors, designed to operate under high temperature and pressure. The reactors were heated in preheated Paratherm HR heat-transfer fluid (Conshohocken, PA). One reactor had a thermometer to provide a representative measurement of the temperature inside all reactors. Experiments were carried out at a solids content of 25%, which was in the same range as reported previously (Rose et al., 2015) and measured in this study (20% ± 5.1%). The dried and homogenized excreta were mixed with double-distilled water to achieve the desired ratio. The experiments were conducted at combinations of different temperatures (180, 210, 240 °C) and reaction times (30, 60, 120 min). Each combination was conducted in triplicate. Reaction time counts started only when the reactor reached the desired temperature, which took between 10 and 25 min.

The treatment temperatures and times were combined into a single parameter, the severity factor, as developed by a coalification model (Ruyter, 1982):

$$f = 50{*}t^{0.2}{*}e^{\frac{-3500}{T}} \quad (1)$$

where t is the reaction time in seconds, and T is the temperature in K. At the end of the desired reaction time, the reactors were placed in an ice bath to immediately suppress the reaction. The produced hydrochar and aqueous phases were separated by centrifuging the slurry for 20 min at 5500 rpm followed by vacuum filtration using a 0.70-μm glass-fiber filter. The impact of reaction severity on the chemical processes and properties of the resulting char and aqueous phases was studied.

2.2. Feedstock and phases properties

This sub-section consists of the different analyses conducted to the two main phases generated by HTC and the raw human excreta. The parts consist of: (1) solid phase analyses, and (2) aqueous phase analyses.

2.2.1. Hydrochar and raw excreta

The wet hydrochar was weighed, dried at 105 °C for 24 h and reweighed. The hydrochar yield was determined by the ratio of the dry weight of the hydrochar to the initial dry weight of the raw excreta. Organic matter and ash contents were determined for both raw excreta and hydrochar by the gravimetric method (APHA, 2005). Elemental composition of carbon, hydrogen, nitrogen and sulfur was conducted with a FlashEA™1112 CHNS-O Analyzer (Thermo Fisher Scientific Inc., UK), while oxygen content was calculated by subtraction of the other elements and ash (ASTM-D3176, 2015). Higher heating values (HHVs) were calculated for both raw excreta and hydrochar (Channiwala and Parikh, 2002), and were validated by bomb calorimeter (data not shown), measured at an ISO-authorized laboratory (Envirolab, Israel). HHVs were used to calculate energetic retention efficiency and energy densification. Fiber analysis measurements of hemicellulose, cellulose and lignin were conducted by an ISO authorized lab (E.H. Smoler Consulting and Research for Agricultural Science Ltd., Israel).

Fourier transform infrared (FTIR) spectroscopy was conducted with a Nicolet 6700 in attenuated total reflectance (ATR) mode equipped with a diamond holder (Thermo Fisher Scientific Inc., UK). The spectrum of each sample was collected in the 600–4000 cm^{-1} region with a spectral resolution of 4 cm^{-1} and 36 scans. Spectra were corrected for background transmittance, atmospheric suppression and ATR correction. FTIR peak identification

was based on the literature (Coates, 2000; He et al., 2013; Reza et al., 2014; Wang et al., 2018; Xu and Chen, 2013). FTIR data processing was performed using OMNIC software (Thermo Fisher Scientific), in the spectral wavelength range of 4000 to 650 cm^{-1}. FTIR spectra were analyzed by principal component analysis (PCA) to better visualize the differences between the treatments. In the PCA, each wavelength measured in the FTIR was considered to be a variable. The variables were reduced to two principal components that accounted for most of the variation in the data. PCA can be helpful in correlating spectral data and chemical behavior. PCA was performed using MATLAB 2016a software (Mathwork, Inc.). A summary table describing all the measured and calculated parameters of this study can be found in Table S1 (supplementary data).

2.2.2. Aqueous phase

Aqueous-phase samples were kept in a freezer (−20 °C) for no more than 2 months prior to their characterization. Samples were analyzed for pH and electrical conductivity (EC) using CyberScan pH11 and Con11 (Eutech Instruments Ptv. Ltd., Singapore), respectively. Total nitrogen (TN) and dissolved organic carbon (DOC) were analyzed with a TOC analyzer (Multi N/C, Analytik-Jena, Germany). Analysis of macro- and micronutrients was conducted by inductively coupled plasma (ICP) analyzer (ICP–AES, Varian 720ES, Australia). Sodium absorption ratio (SAR) was calculated from the measured concentrations of sodium, calcium and magnesium. All analyses followed standard procedures (APHA, 2005).

2.3. Mass balance and energy accounting

Mass balance and energy accounting calculations were conducted followed the protocol by Mau et al. (2016). Briefly, carbon and nitrogen mass balances were calculated for each HTC reaction according to the amount of each material in the solid and aqueous phase according to:

$$m_e \times C_e = m_h \times C_h + m_a \times C_a \quad (2)$$

where m is the mass of the phase and C is the element concentration. The subscripts e, h, and, a denote raw excreta, hydrochar and aqueous phases, respectively.

Energy accounting was determined for each HTC reaction by calculating the input energy, which is the energy required for the HTC process, and the output energy which is the energy produced by the combustion of hydrochar. The input energy (E_{input}) required to heat the sludge was calculated by summing the energy needed to heat the water (E_{water}) and the energy needed to heat the solid phase (E_{solid}) as follows:

$$E_{water} = m_w\left(H_{w,HTC} - H_{w,25}\right) \quad (3)$$

$$E_{solid} = m_s c_p (T_{HTC} - 25) \quad (4)$$

$$E_{input} = E_{water} + E_{solid} \quad (5)$$

where m_w and m_s are the sludge water and solid mass, respectively; $H_{w,HTC}$ and $H_{w,25}$ are the enthalpy of water at the final HTC reaction temperature and at 25 °C, respectively; c_p is the specific heat capacity of dry excreta, 1.7 kJ/kg ºC (Namioka et al., 2008) and T_{HTC} is the reaction temperature. Energy output (E_{output}) was calculated as follows:

$$E_{output} = m_h \cdot \Delta H_c^{\circ} \quad (6)$$

where m_h is the hydrochar mass and ΔH_c° is the heat of combustion expressed by the calorific value (HHV). All calculated values of mass balance and energy accounting were normalized to 1 kg of sludge.

2.4. Pilot scale reactor

Pilot scale experiments were conducted to test for possible differences from the laboratory scale reactors. A 30-L HTC reactor was used (Fig. S1, supplementary data). It is made of stainless steel with inner coating of enamel with a stainless steel cap closed by screws (Düker GmbH, Germany), each tightened with a force of 600 MN. A crane was used to safely lift and lower the cap. The reactor is heated by heat exchange with Paratherm HR heat-transfer fluid (Conshohocken, PA), which is heated in an electrical oil bath attached to a pump. Human excreta was collected from 12 people and dried as previously described in section 2. Two experiments were conducted by heating 2 and 3 kg of dry excreta that was mixed with double distilled water at 1:4 solid-to-water ratio, representing upscaling by 3 orders of magnitude. The slurry was heated to 210 °C for 4 h. Unlike the batch reactor, heating and cooling times were longer due to the reactor size, taking 340–450 min to reach 180 °C. Aqueous phase and hydrochar from the large reactor were collected and separated by centrifuge. Hydrochar and aqueous phase were characterized in a similar manner as described in sections 2.2.1 and 2.2.2, respectively.

2.5. Statistical analysis

Statistical analysis was carried out to determine significant differences between treatments (i.e. reaction temperature and time). Two-way analysis of variance (ANOVA) was carried out at 95% confidence interval. In these analyses, reaction temperature and time were the fixed independent variables, and the measured parameters (described above and in supplementary data) were the dependent variables. One-way ANOVA was also carried out to compare the raw human excreta with hydrochar generated at various temperatures and reaction time of 120 min at 95% confidence interval using temperature as the independent factor. When a significant difference was found, Tukey's post hoc test was run to determine specific differences between groups. The comparison between laboratory and pilot scale reactors was analyzed by Student's t-test at 95% confidence interval. All statistical analyses were conducted using STATISTICA software (StatSoft Inc.)

3. Results and discussion

In the following sub-sections, we present and discuss the result obtained in the HTC experiments. We start with the results from the hydrochar characterization, followed by the aqueous-phase characterization. After that, we focus on mass balance of carbon and nitrogen. Lastly, the energy accounting of the HTC process is considered.

3.1. Hydrochar characterization

Human excreta and the derived hydrochar were characterized for laboratory and pilot scale experiments. This data is essential to better understand the HTC of human excreta process as well as to evaluate potential reuse avenues. Results are presented in four subsections: (1) the physicochemical characterization, (2) a comparison with the pilot scale reactor, (3) the fiber composition, and (4) the functional groups in the material surface by FTIR analysis.

3.1.1. Physical and chemical analyses

Hydrochar yield decreased significantly with temperature ($P < 0.05$) (Table 1and S2, supplementary data). A similar temperature effect has been found for primary sewage sludge (Danso-Boateng et al., 2015a). In another study of human excreta, Afolabi et al. (2017) observed lower yields of about 48% hydrochar produced with 5% solids content at 200 °C, possibly due to the much lower solids content or heating method (oil bath in the present study vs. microwave). Hydrochar moisture content decreased significantly ($P < 0.05$) by 26% after 120 min at 240 °C, indicating an increase in hydrochar hydrophobicity. This result may be explained by reduction of hydrophilic oxygen functional groups (He et al., 2013). A decrease of up to 2.4% of organic matter content was observed, and both temperature and reaction time were significant ($P < 0.05$) factors. The decrease in organic matter can be explained by its transformation from the solid phase to the aqueous and gaseous phases due to chemical reactions such as dehydration and decarboxylation (Funke and Ziegler, 2010).

The hydrochar elemental composition changed as a result of HTC (Table 1and S2, supplementary data). Nitrogen concentration decreased significantly ($P < 0.05$) with time and temperature by up to 2.5%. Danso-Boateng et al. (2015c) and Afolabi et al. (2017) found a similar reduction for primary sewage sludge and human excreta, respectively. Ekpo et al. (2016b) and Heilmann et al. (2014), who investigated poultry manure, found an up to 3% decrease in nitrogen concentration. This decrease was attributed to the degradation of proteins, which make up the main nitrogenous matter in fecal biomass (Rose et al., 2015). No clear trend was found with hydrogen concentration. Carbon concentration increased after carbonization; both time and temperature were significant factors ($P < 0.05$) (Table 1). Oxygen concentration decreased significantly ($P < 0.05$) by 10.4% after 120 min of treatment at 240 °C. The increase in relative carbon content was attributed to the reduction in oxygen and nitrogen concentrations.

The severity factor (Eq. (1)) was highly correlated with carbon content ($R^2 = 0.95$) and calorific value ($R^2 = 0.89$) (Fig. 1). Therefore, it can probably be used to predict carbon content and HHV with different time and temperature combinations within the tested range of severity factors. Model validation with different time and temperature combinations is needed, and for broader applicability, different feedstocks should be investigated as well. It should also be noted that temperature and time affect the end result differently. The severity factor is linearly dependent on time and exponentially dependent on temperature following Arrhenius behavior (Ruyter, 1982).

The feedstock energy retained in the hydrochar is quantified by the energetic retention efficiency. This efficiency decreased with temperature ($P < 0.05$) from 74 (at 180 °C) to 67% (at 240 °C), similar to values found by Afolabi et al. (2017). It should be noted though, that the average calorific value after HTC increased consistently up to 27.6 ± 0.16 MJ/kg after 120 min at 240 °C from that of the raw human excreta (22.9 ± 0.05 MJ/kg). In other words, the quality of the hydrochar as reflected by its densification was higher and was a function of severity (Table 1). The calorific values obtained are within the range for sub-bituminous to bituminous coal (ASTM, 2002).

A Van Krevelen diagram was used to visualize the atomic ratios of hydrogen to carbon (H:C) and oxygen to carbon (O:C) (Fig. 2). This diagram is used to assess and classify different coal groups and kerogen types according to H:C and O:C ratios (Van Krevelen, 1984). The lower the respective ratios are, the greater the energy content and maturity level of the material. In the diagram there are also vectors representing the change in atomic ratios due to dehydration and decarboxylation reactions. These vectors can inform which reaction was more prominent during HTC. As described in Fig. 2, decarboxylation was more pronounced than dehydration. Raw human excreta did not follow the conventional classification of biomass. The H:C ratio was 1.7 and the O:C ratio was 0.4, very similar to the values found by Lu et al. (2017) who investigated hydrothermal liquefaction of human excreta. Furthermore, the resulting hydrochar did not seem to resemble any coal group. A possible explanation is that human excreta contain more fat than other investigated manures and carbonaceous materials. Human excreta have about 8.7–18% fat (Lu et al., 2017; Rose et al., 2015), whereas chicken manure has 1.1–2.1% fat, cow manure has 2.5–8.7% fat, and swine manure has 9.1–9.4% fat (Heilmann et al., 2014; Kafle and Chen, 2016). These findings demonstrate the possible differences between human excreta and other animal manures. After carbonization for 120 min at 240 °C, the hydrochar had an H:C of 1.5 and O:C of 0.2, which was similar to the ratios obtained by He et al. (2013) and Peng et al. (2016) who investigated sewage sludge. There are indications that the higher pH measured in the aqueous phase (see section 3.2) was associated with a higher H:C ratio (Funke and Ziegler, 2010). Moreover, the Van Krevelen

Table 1
Physicochemical characteristics of hydrochar generated by HTC under the specified severity factors resulting from various temperatures and 120 min reaction time. Values are presented as mean ± standard error.

Parameters	Raw human excreta	HTC severity factor		
		0.13 (180 °C)	0.21 (210 °C)	0.32 (240 °C)
Elemental analysis				
H (%)	7.07 ± 0.03[a]	7.28 ± 0.07[ab]	7.08 ± 0.11[a]	7.42 ± 0.02[b]
C (%)	50.25 ± 0.08[a]	53.42 ± 0.53[b]	55.55 ± 0.92[b]	59.66 ± 0.33[c]
O (%)	25.85 ± 0.08[a]	20.67 ± 0.41[ab]	19.25 ± 0.95[ab]	15.46 ± 0.15[b]
N (%)	4.51 ± 0.17[a]	4.69 ± 0.24[a]	3.38 ± 0.10[b]	2.96 ± 0.20[b]
S (%)	0.06 ± 0.03[ab]	0.16 ± 0.05[b]	0.08 ± 0.00[ab]	0.00 ± 0.00[a]
Proximate analysis				
Organic matter (%)	87.75 ± 0.19[a]	86.22 ± 0.02[b]	85.35 ± 0.05[c]	85.49 ± 0.08[c]
Ash (%)	12.25 ± 0.19[a]	13.78 ± 0.02[b]	14.65 ± 0.05[c]	14.51 ± 0.08[c]
Moisture (%)	80.70 ± 1.17[a]	70.19 ± 0.32[b]	68.01 ± 0.02[c]	54.22 ± 0.37[d]
HHV (MJ/kg)	22.88 ± 0.05[a]	24.74 ± 0.31[b]	25.39 ± 0.55[b]	27.62 ± 0.16[c]
Hydrochar yield (%)[a]		69.19 ± 0.09[a]	64.93 ± 0.54[b]	55.57 ± 0.35[c]
Energetic retention efficiency (%)[b]		74.82 ± 0.85[a]	72.06 ± 1.55[a]	67.04 ± 0.50[b]
Energy densification[c]		1.08 ± 0.01[a]	1.10 ± 0.02[a]	1.21 ± 0.01[b]

[a, b, c, d] Different letters in a row indicate statistically significant difference at 0.05.
[a] (Mass of dry hydrochar/mass of initial raw feedstock) x 100.
[b] (Mass of dry hydrochar x HHV hydrochar)/(mass of initial raw feed stock x HHV feedstock) x100.
[c] (HHV hydrochar)/(HHV feedstock).

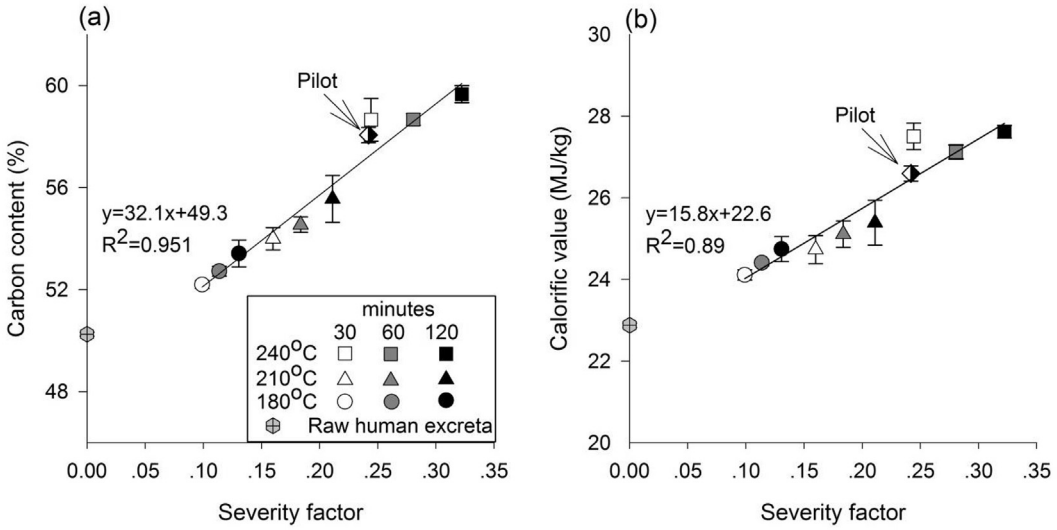

Fig. 1. Correlation between HTC severity factor and (a) carbon content, (b) calorific value after carbonization of human excreta at the specified temperatures and reaction times. Pilot experiment conducted at 210 °C and 240 min is also shown.

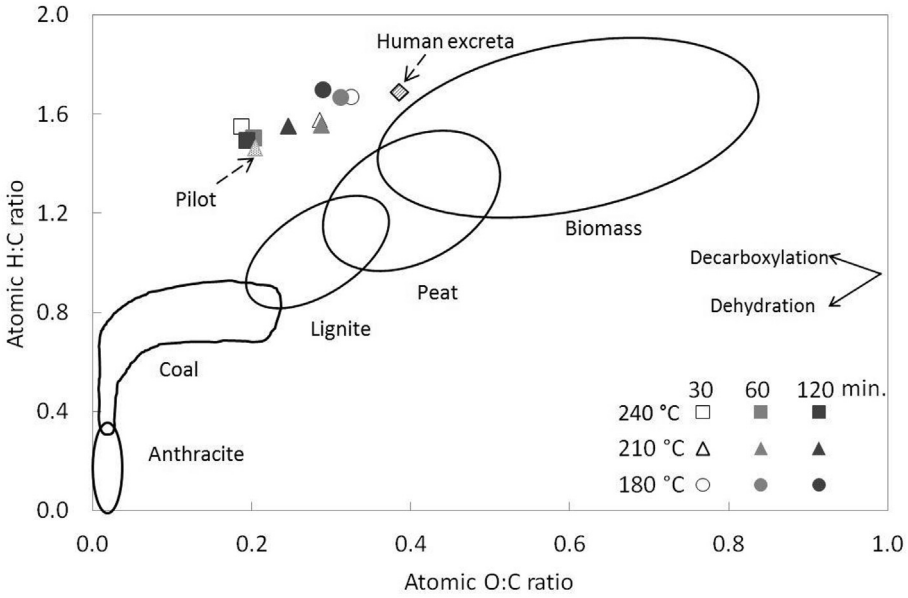

Fig. 2. Van Krevelen diagram of hydrochar produced by HTC at the specified temperatures and times from human excreta with a solid-to-water ratio of 1:4. Pilot experiment conducted at 210 °C and 240 min is also shown. Standard errors are small, ranging from 0.002 to 0.020 for atomic H:C ratio and 0.001–0.012 for atomic O:C ratio.

diagrams presented by Ramke et al. (2009) and Poerschmann et al. (2015) indicate that the hydrochar's O:C and H:C ratios fall under the classification of oil shale or since it is derived from excreta it can be termed biocrude. The latter was shown to be produced during HTC of various feed stocks and it can be separated (extracted) from the hydrochar (Ekpo et al., 2016b). Since such an extraction was not performed in the present study, any biocrude that was generated was present in the hydrochar, conferring oil shale characteristics. This aspect should be further investigated but was beyond the scope of this research.

3.1.2. Pilot scale reactor

The hydrochar produced in the pilot scale reactor had a severity factor of 0.24 resulting from heating at 210 °C for 240 min, achieving the same severity factor as the hydrochar produced in laboratory scale reactor at 240 °C and 30 min. Interestingly, both hydrochars obtained similar physicochemical properties (Table S3, supplementary data, Figs. 1–2) suggesting that there was no distinct effect to the reactor size. The hydrochar yield was smaller and it was likely an artifact due to the difficulty to scrap and collect all the hydrochar from the pilot scale reactor. Similar results were also found when comparing properties of the aqueous phase between the laboratory and pilot reactors except for DOC and potassium concentrations (Table S3, supplementary data). The latter, however, were in the in the same order of magnitude. These results indicate that the knowledge gathered in laboratory experiments can be assumed representative if conducted in larger operations. This is essential in bridging the gap from research to application of HTC.

3.1.3. Fiber analysis

In general, the various components of biomass possess calorific values in the following ascending order: ash < hemicellulose < cellulose < lignin (Reza et al., 2013). This order is congruous with each compound's temperature of hydrolysis. Hemicellulose decomposition to monomers of glucose and other sugars begins at approximately 180 °C, whereas decomposition of cellulose begins between 200 and 220 °C or above. Lignin is the most complex, and a higher temperature of approximately 250 °C is needed for its decomposition (Funke and Ziegler, 2010; Kim et al., 2016). Fiber analyses demonstrated that the percent concentration of the three components in the raw excreta is similar, ranging from 12 to 16 (Fig. 3). As expected, at 180 °C, hemicellulose showed the most pronounced decomposition and a reduction of approximately 10% was observed. Minor decomposition of cellulose was noted, while the lignin fraction remained unchanged. There were technical problems with the analysis of hemicellulose at 240 °C, and it is therefore not shown.

3.1.4. Fourier transform infrared spectroscopy analysis

FTIR was used to determine the relative presence of different functional groups in the raw human excreta and the hydrochar (Fig. S2, supplementary data). By comparing them, carbonization progress was evaluated. The peaks centered around 3315 cm^{-1} and 1650 cm^{-1} corresponding to −OH stretching vibrations of hydroxyl or carboxyl, and C=O stretching vibrations in ketone and amide groups significantly decreased in intensity with increased treatment severity. The reduction of these peaks is related to dehydration and decarboxylation reactions, respectively. The reduction in −OH functional groups, associated with increased hydrophobicity (Funke and Ziegler, 2010), explains the decrease in hydrochar moisture (section 3.1.1). The reduction in C=O is corroborated by the decrease in oxygen concentration (Table 1). Interestingly, a new peak at 1705 cm^{-1} appeared in the spectra of all hydrochars. This may correspond to a ketone functional group, indicating the presence of functional groups that contain oxygen on the hydrochar surface.

The carbonization progression was evident in the disappearance of the peaks at 1735 cm^{-1} and 1550 cm^{-1}. These peaks are attributed to C=O stretching vibrations in hemicellulose and the amide (−NH) vibrations. The C=O is already absent in the spectra of 180 °C hydrochar, likely a reflection of hemicellulose decomposition at this temperature. The −NH peak was sharply reduced at 180 °C and disappeared completely at 210 °C. This reduction likely indicates protein degradation during the carbonization process.

Lastly, the intensity of the peaks at 2925 cm^{-1}, 2850 cm^{-1}, and 1465 cm^{-1} remained relatively constant. The 2925 cm^{-1} and 2850 cm^{-1} peaks were attributed to asymmetric and symmetric −C−H stretching of methylene groups (−CH2−) within larger molecules in the hydrochar. The peak at 1465 cm^{-1} was attributed to C−H band stretching of lignin, demonstrating that there was no major decomposition of lignin. These results coincide with the findings of the fiber analysis (Fig. 3).

PCA was performed to better analyze the FTIR spectra. The PCA explained 90% of the total variation between samples, where PC1 = 68.1%, and PC2 = 21.9%. Since PC1 can explain most of the variation, it was correlated to the severity factor and a good correlation ($R^2 = 0.934$) between the two was found (Fig. S3, supplementary data). The PCA supported the notion that the FTIR spectra demonstrate a clear progression of carbonization intensity with increasing HTC treatment temperature and time. As with carbon content and HHV, temperature had a more significant effect than time and governed the carbonization process.

3.2. Aqueous-phase characterization

Previous studies indicate that the aqueous phase has the greatest environmental impact of all the components in the HTC life cycle (Benavente et al., 2017; Berge et al., 2015). Thus, its efficient utilization is of interest. Analyses of the aqueous phase enable a better understanding of the HTC process and may shed light on its potential usage (e.g. for fertilization). The aqueous phase characteristics changed in both color and odor with increasing treatment severity. It acquired a darker brown−black color and had a coffee-like smell, suggesting that Maillard reactions had occurred. During the Maillard reaction, amino acids and reduced sugars interact to produce soluble products, such aldehydes, furans, pyrazines and pyridines, while the end product has a different color and smell (Danso-Boateng et al., 2015c).

The aqueous phase's physicochemical properties are summarized in Table 2 and S4 (supplementary data). A markedly high DOC concentration was found in the aqueous phase prior to HTC, due to the high solubility of feces and the presence of urine in the excreta. On average, urine contains 2350−6550 mg/L carbon (Rose et al.,

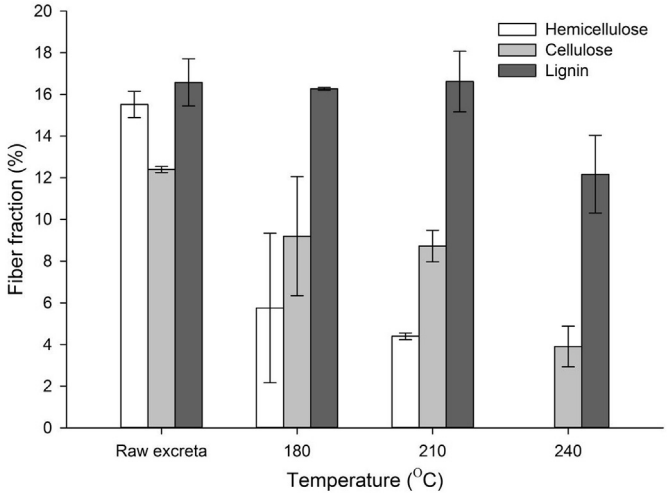

Fig. 3. Fiber analysis of cellulose, hemicellulose and lignin after carbonization of human excreta at the specified temperatures for 120 min.

Table 2
Characterization of aqueous phase generated by HTC under the specified severity factors resulting from various temperatures and 120 min reaction time. Values are presented as mean ± standard error.

Parameters	Raw human excreta	HTC severity factor		
		0.13 (180 °C)	0.21 (210 °C)	0.32 (240 °C)
pH	6.2 ± 0.0^{a}	5.4 ± 0.1^{b}	6.1 ± 0.1^{a}	7.4 ± 0.0^{c}
EC (mS/cm)	15.5 ± 0.4^{a}	23.6 ± 0.1^{ab}	25.8 ± 0.4^{ab}	29.9 ± 1.4^{b}
DOC (g/L)	25.3 ± 0.9^{a}	40.7 ± 3.7^{b}	35.2 ± 3.2^{b}	36.4 ± 5.0^{b}
TN (mg/L)	4187 ± 400^{a}	7801 ± 648^{b}	8718 ± 489^{b}	7908 ± 1501^{b}
P (mg/L)	982 ± 30^{a}	1188 ± 45^{b}	380 ± 11^{c}	71 ± 8^{d}
K (mg/L)	4160 ± 79^{a}	5707 ± 182^{b}	6018 ± 271^{b}	5585 ± 94^{b}
Ca (mg/L)	51 ± 3^{a}	11 ± 1^{b}	5 ± 0^{b}	11 ± 2^{b}
Mg (mg/L)	395 ± 10^{c}	800 ± 28^{d}	272 ± 19^{a}	85 ± 7^{b}
S (mg/L)	448 ± 22^{a}	781 ± 35^{b}	798 ± 51^{b}	658 ± 20^{b}
Fe (mg/L)	4 ± 0^{a}	17 ± 1^{d}	10 ± 0^{c}	7 ± 0^{b}
Na (mg/L)	1432 ± 25^{a}	1942 ± 62^{b}	2123 ± 71^{b}	1880 ± 60^{b}
NPK ratio[a]	2.1:1:2.2	3:1:2.5	8.4:1:8.4	47.8:1:42.6
SAR[b]	15 ± 0^{a}	15 ± 0^{a}	27 ± 1^{b}	47 ± 6^{c}

[a, b, c] Different letters in a row indicate statistically significant difference at 0.05.
[a] $N:P(P_2O_5):K(K_2O)$ ratio on a dry weight basis.
[b] $Na^{+}/(0.5(Ca^{2+} + Mg^{2+}))^{0.5}$ where all concentrations are in meq/L.

2015). There was an increase in DOC after carbonization, peaking at 180 °C ($P < 0.05$; Table 2). These results indicate transformation of carbon from the solid to aqueous phase. Lower DOC values of 6.8–9 g/L were obtained in previous studies (Afolabi et al., 2015; Danso-Boateng et al., 2015c). When correcting for the higher dilution (solid-to-water ratio of about 1:19), the values become similar to those found here.

Initial TN concentration was quite high (Table 2), due to the presence of urea in the urine. Typically, nitrogen concentration in urine ranges between 4000 and 14,000 mg/L (Rose et al., 2015). After HTC, TN concentrations were significantly higher (Table 2). Since dry human feces contain 2–25% TN (dry weight), mostly in the form of proteins (Rose et al., 2015), the increase was likely due to their degradation. A similar trend was obtained previously for swine manure at temperatures of up to 200 °C, although no statistical analysis was reported (Ekpo et al., 2016a).

TN concentration in the aqueous phase increased with reaction time more than with temperature ($P < 0.05$) reaching a concentration of about 8000 mg/L after 120 min at all temperatures (Table S4, supplementary data). In the current study, the different nitrogen fractions were not characterized, but a few previous studies have indicated that most of the TN is organic (75%) (Ekpo et al., 2016b). Nevertheless, as the temperature increases, more of the organic fraction turns into ammonia (Ekpo et al., 2016a; He et al., 2015).

In the present study, initial pH was 6.2. After carbonization at 180 °C, the pH decreased to 5.4 (Table 2), probably due to the presence of organic acids from the decomposition of cellulosic biomass (Hoekman et al., 2011; Mau et al., 2016). The increase in pH with carbonization at the higher temperatures (210 °C and 240 °C) was probably due to production of ammonium-N and degradation of the acidic compounds produced at lower temperatures (Ekpo et al., 2016b; Mumme et al., 2011).

Dissolved phosphorus concentration increased with HTC at 180 °C compared to the untreated aqueous phase (Table 2). At higher HTC temperatures, it decreased. The same trend was observed for magnesium (Table 2). Phosphorus has been shown to react with multivalent metals such as calcium, magnesium, and iron present in manures to form insoluble phosphate (Heilmann et al., 2014). Although not directly measured, it is likely that phosphorus precipitated from the aqueous phase as magnesium phosphate with increasing carbonization temperature and pH (Dai et al., 2015).

Potassium concentration increased significantly after HTC (Table 2). Interestingly, at all of the tested temperatures, the N:P:K ratios were similar to those of different commercial fertilizers (www.icl-sf.com/explore/fruit-vegetables-arable-crops/fertigation-fertilizers/) suggesting its potential use as a fertilizer.

Following HTC, salinity, as expressed by EC, increased significantly from the initial aqueous phase (Table 2). Results are similar in trend to previous studies (e.g. Mau et al., 2016). SAR is used in agriculture to estimate the suitability of water for irrigation and is related to the relative concentration of sodium (monovalent ion) to calcium and magnesium (divalent ions) (Oster, 1994). A SAR of up to 4–5 meq/L is allowed for unlimited irrigation by various standards (e.g., Australian and New Zealand Environment and Conservation Council and the Agriculture and Resource Management Council of Australia and New Zealand, 2000; Inbar, 2007). SAR values after 120 min at 240 °C were much higher than would be allowed for direct irrigation, mainly due to the high sodium concentration, whereas magnesium concentration decreased significantly after carbonization at 240 °C and calcium concentration remained consistently low (Table 2). Despite the high levels of SAR and EC, considering the dilution (i.e., >50 dilution factor) needed to reach appropriate nutrient concentrations, both salinity and SAR would be reduced to concentrations that are suitable for agriculture. Use of the aqueous phase for fertilization has been suggested, but its actual application has scarcely been investigated and requires further research.

3.3. Mass balances

Total carbon recovery rates were 97%, 92% and 82% for HTC at 180, 210 and 240 °C, respectively. Mass balance indicated that most of the carbon was retained in the solid phase, but there was a decrease in its content with increasing temperatures: 80%, 70%, 65% and 55% in raw excreta, and after 180, 210 and 240 °C, respectively (Fig. 4a). The aqueous-phase accounted for 26–28% of the carbon and was similar at all temperatures. These results are consistent with Danso-Boateng et al. (2013) who investigated primary sewage sludge at up to 200 °C. The remaining missing 3–18% of the carbon was probably present in the gaseous phase, which was not characterized in this study. However, similar findings of 2–11% carbon in the gaseous phase, mainly in the form of carbon dioxide, have been reported (Berge et al., 2011; Hoekman et al., 2011; Koottatep et al., 2016).

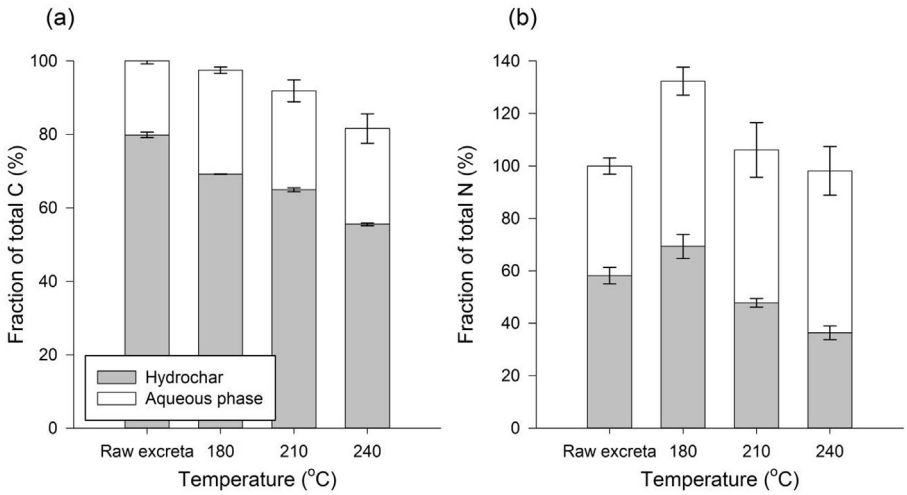

Fig. 4. Mass balance of (a) carbon and (b) nitrogen for human excreta after carbonization for 120 min at the specified temperatures.

Table 3
Energy accounting for carbonization at the specified temperatures for 120 min. Values are presented as mean ± standard error.

Temperature (ºC)	Energy input (kJ/kg sludge)			E_{output} (kJ/kg sludge)	E_{input}/E_{output} (%)
	E_{water}	E_{solid}	E_{input}		
180	527	53	579	3423 ± 39	17
210	634	63	697	3297 ± 71	21
240	746	73	819	3067 ± 23	27

Analysis of the nitrogen mass balance indicated an almost equal concentration of nitrogen between the solid and aqueous phases prior to carbonization (Fig. 4b). After carbonization, there was a transformation of 11% (210 °C) to 22% (240 °C) nitrogen from the solid to the aqueous phase. As discussed in section 3.2, this transformation resulted from the decomposition of organic nitrogen compounds, mainly proteins, which hydrolyzed to amino acids and ammonium (Afolabi et al., 2015; Wang et al., 2018). Overall, the nitrogen in the aqueous and solid phases accounted for 98 ± 12% (210 °C) to 106 ± 12% (240 °C), suggesting that the gaseous nitrogen fraction was insignificant. Although not measured in the study, this coincides with previous results on insignificant nitrogen gas emission following HTC (Mau et al., 2016). It should be noted that the results of the solid nitrogen fraction after carbonization at 180 °C were significantly higher than expected, with no apparent explanation, and thus were not considered. Unfortunately, we did not have enough samples to repeat this analysis.

3.4. Energy accounting

The energy accounting for HTC after 120 min is summarized in Table 3. The increase in total energy requirements for HTC at 240 °C vs. 180 °C (Table 3) was mostly due to the energy needed to heat the water to the higher temperature. The reduction in energy output in the hydrochar (reported as kg sludge) at 240 °C vs. 180 °C (Table 3) was due to carbon loss as the carbonization temperature increased. However, the carbon density in the hydrochar was higher as the temperature increased, resulting in a higher calorific value per gram of char, which is desirable (as discussed in section 3.1.1). The overall analysis suggested that the energy demand for HTC is only 17–27% of the energy output in the hydrochar. Note that the energy demand does not take into consideration either the energy needed to heat the reactor or heat losses during the process. In the current study, a solid-to-water ratio of 1:4 was used, but lower ratios should be investigated as they may result in lower energy demand. The significance of the solid-to-water ratio to the overall energy accounting has been emphasized in previous studies (Danso-Boateng et al., 2015a; Mau et al., 2016).

4. Conclusions

Raw human excreta were studied under different HTC reaction severities in laboratory and pilot scale reactors with no distinct effect to the reactor size. Interestingly, raw human excreta did not follow the conventional classification of biomass in terms of its H:C and O:C elemental ratios. Moreover, following HTC, the resulting hydrochar did not resemble elemental ratio classification of coal but was closer to oil shale. The calorific value ranged from 24.7 to 27.6 MJ/kg, and had enough energy to potentially be used as an energy source. The severity factor was well correlated with carbon content and calorific value, and can be used for their prediction. Further investigation on the hydrochar combustion properties and environmental impact are needed. The aqueous phase contained high nutrient concentrations and can potentially be used as a liquid fertilizer. Yet, its applicability should be validated in the field. This study has provided indications that HTC could be a sustainable sanitation treatment for raw human excreta due to its potential closed-loop cycle approach that recovers energy and enables the reuse of nutrients.

Acknowledgements

This study was funded by the Rosenzweig-Coopersmith Foundation (USA) and the Israeli Water Authority. The authors would like to thank, Drs. Frits Caspers, Beatrice Bressan and Sergio Bertolucci from the European Organization for Nuclear Research (CERN, Switzerland) and Dr. Yaakov Garb (Ben Gurion University) for assisting with the pilot scale reactor design and donation. From Ben Gurion University, we also thank Dr. Itamar Giladi for helping with the statistical analysis, Drs. Sofiya Kolusheva, Roni Kasher and Amos Russak for their assistance with the analytics. Lastly we thank Paratherm for donating the heat-transfer fluid used in this research.

Appendix A. Supplementary data

Supplementary data to this article can be found online at https://doi.org/10.1016/j.jclepro.2018.09.126.

References

Afolabi, O.O.D., Sohail, M., Thomas, C.L.P., 2017. Characterization of solid fuel chars recovered from microwave hydrothermal carbonization of human biowaste. Energy 134, 74–89. https://doi.org/10.1016/j.energy.2017.06.010.
Afolabi, O.O.D., Sohail, M., Thomas, C.P.L., 2015. Microwave hydrothermal carbonization of human biowastes. Waste Biomass Valorization 6, 147–157. https://doi.org/10.1007/s12649-014-9333-4.
APHA, 2005. Standard Methods for the Examination of Water and Wastewater, twenty-first ed. American Public Health Association, Washington.
ASTM-D3176, 2015. Standard practice for ultimate analysis of coal and coke. Annu. Book ASTM Stand. 1–4. https://doi.org/10.1520/D3176-15.2.
ASTM, C.D.-5, 2002. Standard classification of coals by rank. Annu. Book ASTM Stand. 1–7. https://doi.org/10.1520/D0388-12.2, 05.06. 05.
Australian and New Zealand Environment and Conservation Council and the Agriculture and Resource Management Council of Australia and New Zealand, 2000. ANZ Guidelines for Fresh and Marine Water Quality - Primary Industries - Rationale and Background Information, vol. 3, p. 264 (Canberra, Australia).
Bailis, R., Ezzati, M., Kammen, D.M., 2003. Greenhouse gas implications of household energy technology in Kenya. Environ. Sci. Technol. 37, 2051–2059. https://doi.org/10.1021/es026058q.
Benavente, V., Fullana, A., Berge, N.D., 2017. Life cycle analysis of hydrothermal carbonization of olive mill waste: comparison with current management approaches. J. Clean. Prod. 142, 2637–2648. https://doi.org/10.1016/j.jclepro.2016.11.013.
Berge, N.D., Li, L., Flora, J.R.V., Ro, K.S., 2015. Assessing the environmental impact of energy production from hydrochar generated via hydrothermal carbonization of food wastes. Waste Manag. 43, 203–217. https://doi.org/10.1016/j.wasman.2015.04.029.
Berge, N.D., Ro, K.S., Mao, J., Flora, J.R.V., Chappell, M.A., Bae, S., 2011. Hydrothermal carbonization of municipal waste streams. Environ. Sci. Technol. 45, 5696–5703. https://doi.org/10.1021/es2004528.
Channiwala, S. a., Parikh, P.P., 2002. A unified correlation for estimating HHV of solid, liquid and gaseous fuels. Fuel 81, 1051–1063. https://doi.org/10.1016/S0016-2361(01)00131-4.
Coates, J., 2000. Interpretation of infrared spectra , a practical approach interpretation of infrared spectra , a practical approach. Encycl. Anal. Chem. 10815–10837. https://doi.org/10.1002/9780470027318.
Dai, L., Tan, F., Wu, B., He, M., Wang, W., Tang, X., Hu, Q., Zhang, M., 2015. Immobilization of phosphorus in cow manure during hydrothermal carbonization. J. Environ. Manag. 157, 49–53. https://doi.org/10.1016/j.jenvman.2015.04.009.
Danso-Boateng, E., Holdich, R.G., Martin, S.J., Shama, G., Wheatley, A.D., 2015a.

Process energetics for the hydrothermal carbonisation of human faecal wastes. Energy Convers. Manag. 105, 1115–1124. https://doi.org/10.1016/j.enconman.2015.08.064.
Danso-Boateng, E., Holdich, R.G., Shama, G., Wheatley, A.D., Sohail, M., Martin, S.J., 2013. Kinetics of faecal biomass hydrothermal carbonisation for hydrochar production. Appl. Energy 111, 351–357. https://doi.org/10.1016/j.apenergy.2013.04.090.
Danso-Boateng, E., Holdich, R.G., Wheatley, A.D., Martin, S.J., Shama, G., 2015b. Hydrothermal carbonization of primary sewage sludge and synthetic faeces: effect of reaction temperature and time on filterability. Environ. Prog. Sustain. Energy 34, 1279–1290. https://doi.org/10.1002/ep.12114.
Danso-Boateng, E., Shama, G., Wheatley, A.D., Martin, S.J., Holdich, R.G., 2015c. Hydrothermal carbonisation of sewage sludge: effect of process conditions on product characteristics and methane production. Bioresour. Technol. 177, 318–327. https://doi.org/10.1016/j.biortech.2014.11.096.
Ekpo, U., Ross, A.B., Camargo-Valero, M.A., Fletcher, L.A., 2016a. Influence of pH on hydrothermal treatment of swine manure: impact on extraction of nitrogen and phosphorus in process water. Bioresour. Technol. 214, 637–644. https://doi.org/10.1016/j.biortech.2016.05.012.
Ekpo, U., Ross, A.B., Camargo-Valero, M.A., Williams, P.T., 2016b. A comparison of product yields and inorganic content in process streams following thermal hydrolysis and hydrothermal processing of microalgae, manure and digestate. Bioresour. Technol. 200, 951–960. https://doi.org/10.1016/j.biortech.2015.11.018.
Escala, M., Zumbühl, T., Koller, C., Junge, R., Krebs, R., 2013. Hydrothermal carbonization as an energy-efficient alternative to established drying technologies for sewage sludge: a feasibility study on a laboratory scale. Energy Fuels 27, 454–460. https://doi.org/10.1021/ef3015266.
Funke, A., Ziegler, F., 2010. Hydrothermal carbonization of biomass: a summary and discussion of chemical mechanisms for process engineering. Biofuels Bioprod. Biorefining 4, 160–177. https://doi.org/10.1002/bbb.198.
He, C., Giannis, A., Wang, J.Y., 2013. Conversion of sewage sludge to clean solid fuel using hydrothermal carbonization: hydrochar fuel characteristics and combustion behavior. Appl. Energy 111, 257–266. https://doi.org/10.1016/j.apenergy.2013.04.084.
He, C., Wang, K., Yang, Y., Amaniampong, P.N., Wang, J.Y., 2015. Effective nitrogen removal and recovery from dewatered sewage sludge using a novel integrated system of accelerated hydrothermal deamination and air stripping. Environ. Sci. Technol. 49, 6872–6880. https://doi.org/10.1021/acs.est.5b00652.
Heilmann, S.M., Molde, J.S., Timler, J.G., Wood, B.M., Mikula, A.L., Vozhdayev, G.V., Colosky, E.C., Spokas, K.A., Valentas, K.J., 2014. Phosphorus reclamation through hydrothermal carbonization of animal manures. Environ. Sci. Technol. 48, 10323–10329. https://doi.org/10.1021/es501872k.
Hoekman, S.K., Broch, A., Robbins, C., 2011. Hydrothermal carbonization (HTC) of lignocellulosic biomass. Energy Fuels 25, 1802–1810. https://doi.org/10.1021/ef101745n.
Hu, M., Fan, B., Wang, H., Qu, B., Zhu, S., 2016. Constructing the ecological sanitation: a review on technology and methods. J. Clean. Prod. 125, 1–21. https://doi.org/10.1016/j.jclepro.2016.03.012.
Inbar, Y., 2007. New Standards for Treated Wastewater Reuse in Israel. In: Zaidi, M.K. (Ed.), Wastewater Reuse–Risk Assessment, Decision-Making and Environmental Security. Springer Netherlands, Dordrecht, pp. 291–296. https://doi.org/10.1007/978-1-4020-6027-4_30.
Kafle, G.K., Chen, L., 2016. Comparison on batch anaerobic digestion of five different livestock manures and prediction of biochemical methane potential (BMP) using different statistical models. Waste Manag. 48, 492–502. https://doi.org/10.1016/j.wasman.2015.10.021.
Kim, D., Lee, K., Park, K.Y., 2016. Upgrading the characteristics of biochar from cellulose, lignin, and xylan for solid biofuel production from biomass by hydrothermal carbonization. J. Ind. Eng. Chem. 42, 95–100. https://doi.org/10.1016/j.jiec.2016.07.037.
Koottatep, T., Fakkaew, K., Tajai, N., Pradeep, S.V., Polprasert, C., 2016. Sludge stabilization and energy recovery by hydrothermal carbonization process. Renew. Energy 99, 978–985. https://doi.org/10.1016/j.renene.2016.07.068.
Lu, J., Zhang, J., Zhu, Z., Zhang, Y., Zhao, Y., Li, R., Watson, J., Li, B., Liu, Z., 2017. Simultaneous production of biocrude oil and recovery of nutrients and metals from human feces via hydrothermal liquefaction. Energy Convers. Manag. 134, 340–346. https://doi.org/10.1016/j.enconman.2016.12.052.
Mau, V., Quance, J., Posmanik, R., Gross, A., 2016. Phases' characteristics of poultry litter hydrothermal carbonization under a range of process parameters. Bioresour. Technol. 219, 632–642. https://doi.org/10.1016/j.biortech.2016.08.027.
Mumme, J., Eckervogt, L., Pielert, J., Diakité, M., Rupp, F., Kern, J., 2011. Hydrothermal carbonization of anaerobically digested maize silage. Bioresour. Technol. 102, 9255–9260. https://doi.org/10.1016/j.biortech.2011.06.099.
Namioka, T., Miyazaki, M., Morohashi, Y., Umeki, K., Yoshikawa, K., 2008. Modeling and analysis of batch-type thermal sludge pretreatment for optimal design. J. Environ. Eng. 3, 170–181. https://doi.org/10.1299/jee.3.170.
Oster, J.D., 1994. Irrigation with poor quality water. Agric. Water Manag. 25, 271–297. https://doi.org/10.1016/0378-3774(94)90064-7.
Peng, C., Zhai, Y., Zhu, Y., Xu, B., Wang, T., Li, C., Zeng, G., 2016. Production of char from sewage sludge employing hydrothermal carbonization: char properties, combustion behavior and thermal characteristics. Fuel 176, 110–118. https://doi.org/10.1016/j.fuel.2016.02.068.
Poerschmann, J., Weiner, B., Wedwitschka, H., Zehnsdorf, A., Koehler, R., Kopinke, F.D., 2015. Characterization of biochars and dissolved organic matter phases obtained upon hydrothermal carbonization of Elodea nuttallii. Bioresour. Technol. 189, 145–153. https://doi.org/10.1016/j.biortech.2015.03.146.
Ramke, H., Blöhse, D., Lehmann, H., Fettig, J., 2009. Hydrothermal carbonization of organic waste. In: Twelfth Int. Waste Manag. Landfill Symp (Hoexter, Germany).
Reißmann, D., Thrän, D., Bezama, A., 2018. Hydrothermal processes as treatment paths for biogenic residues in Germany: a review of the technology, sustainability and legal aspects. J. Clean. Prod. 172, 239–252. https://doi.org/10.1016/j.jclepro.2017.10.151.
Reza, M.T., Lynam, J.G., Uddin, M.H., Coronella, C.J., 2013. Hydrothermal carbonization: fate of inorganics. Biomass Bioenergy 49, 86–94. https://doi.org/10.1016/j.biombioe.2012.12.004.
Reza, M.T., Uddin, M.H., Lynam, J.G., Coronella, C.J., 2014. Engineered pellets from dry torrefied and HTC biochar blends. Biomass Bioenergy 63, 229–238. https://doi.org/10.1016/J.BIOMBIOE.2014.01.038.
Rose, C., Parker, A., Jefferson, B., Cartmell, E., 2015. The characterization of feces and urine: a review of the literature to inform advanced treatment technology. Crit. Rev. Environ. Sci. Technol. 45, 1827–1879. https://doi.org/10.1080/10643389.2014.1000761.
Ruyter, P., 1982. Coalif ication model *. Fuel 61, 1182–1187.
Smith, A.M., Singh, S., Ross, A.B., 2016. Fate of inorganic material during hydrothermal carbonisation of biomass: influence of feedstock on combustion behaviour of hydrochar. Fuel 169, 135–145. https://doi.org/10.1016/j.fuel.2015.12.006.
UNICEF, WHO, 2017. Progress on Drinking Water, Sanitation and Hygiene. https://doi.org/10.1111/tmi.12329 (Geneva, Switzerland).
Van Krevelen, D.W., 1984. Organic geochemistry-old and new. Org. Geochem. 6, 1–10. https://doi.org/10.1016/0146-6380(84)90021-4.
vom Eyser, C., Palmu, K., Schmidt, T.C., Tuerk, J., 2015. Pharmaceutical load in sewage sludge and biochar produced by hydrothermal carbonization. Sci. Total Environ. 537, 180–186. https://doi.org/10.1016/j.scitotenv.2015.08.021.
Wang, T., Zhai, Y., Zhu, Y., Peng, C., Xu, B., Wang, T., Li, C., Zeng, G., 2018. Influence of temperature on nitrogen fate during hydrothermal carbonization of food waste. Bioresour. Technol. 247, 182–189. https://doi.org/10.1016/j.biortech.2017.09.076.
Ward, B.J., Yacob, T.W., Montoya, L.D., 2014. Evaluation of solid fuel char briquettes from human waste. Environ. Sci. Technol. 48, 9852–9858. https://doi.org/10.1021/es500197h.
Xu, Y., Chen, B., 2013. Investigation of thermodynamic parameters in the pyrolysis conversion of biomass and manure to biochars using thermogravimetric analysis. Bioresour. Technol. 146, 485–493. https://doi.org/10.1016/J.BIORTECH.2013.07.086.